THE ANALYSIS AND DESIGN OF TRANSONIC

TWO-ELEMENT AIRFOIL SYSTEMS*

G. Volpe and B. Grossman
Grumman Aerospace Corporation

INTRODUCTION

.This paper describes the multiphase effort in the development of tools for the analysis and design of two-element airfoil systems -- that is, airfoils with a slat or a flap at transonic speeds. The first phase involved the development of a method to compute the inviscid flow over such configurations. In the second phase the inviscid code was coupled to a boundary layer calculation program in order to compute the loss in performance due to viscous effects. In the third phase, which is currently in progress, an inverse code that constructs the airfoil system corresponding to a desired pressure distribution is to be developed. The symbols are defined in an appendix.

TWO-ELEMENT AIRFOIL ANALYSIS

The methodology used to compute the inviscid flow over two-element airfoil systems has been described in previous reports (ref. 1-3). It will be summarized here only briefly. The flow field over such configurations is obtained by mapping the doubly connected physical domain into an annulus. The transformation itself follows from the work of Ives (ref. 4), and it is the result of five sequential mappings. The first, a Karman-Trefftz transformation, opens up the main airfoil into a near circle; the second turns the near circle into a perfect one. Then the second airfoil is opened up and transferred to the interior of the main circle. Finally, the second foil is mapped into a circle while managing to retain the shape of the first circle. With this transformation the entire physical space is mapped into the annular region between the two circles with infinity becoming a single point betr en them.

The governing equations for the inviscid, ir . u tional compressible flow are written in this computational domain using the metric of the mapping. A potential function is then introduced to reduce the number of equations to one. The mapping introduces several singularities in the potential equation, but since the mapping is analytic and the transformation is known everywhere, the singularities can be removed analytically. The metric of the transformation is thus normalized with its value at the infinity point, and terms corresponding

to the free stream and the circulatory flows around each element are
subtracted from the potential function. The result is a second-order partial
differential equation for a reduced potential function, which is continuous
and single-valued everywhere. As usual in transonic flow problems the equation
is of mixed type and is solved numerically. The boundary conditions imposed
are, of course, that the normal component of velocity be zero at each surface.
The equation contains two circulation constants that are evaluated by
applying the Kutta condition at each trailing edge.

In the computational domain a simple polar coordinate system emanating
from the center of the annulus automatically generates an orthogonal grid
in which both airfoils lie along grid lines. An accurate application of the
boundary conditions is then made in a relatively straightforward manner. As
described in reference 2, an additional stretching is used to concentrate
points near the leading and trailing edges of both elements and to place both
trailing edge points and the point of infinity exactly at grid points. The
numerical procedure employs standard relaxation techniques along with a non-
conservative, type-dependent, rotated difference scheme. To make sure that
the field is never swept at more than 90° from the streamline direction, the
computational domain is divided into four regions along the ring going through
the infinity point, as shown in figure 1, and then the region over each
of the airfoil surfaces is swept from the leading edge to the trailing edge.
Figure 2 shows a typical computational grid as it appears in the physical
plane. The appropriate high level of concentration of mesh points is obtained
near the leading and trailing edges and in the gap.

The configuration shown in figure 2 is a classic one, and the results of
a computation for a Mach number of 0.6 and an angle of attack of 6° are given
in Figure 3. Very large supersonic regions can be seen to be present on both
elements. These are evident in figure 4, which gives the sonic line along
with some computed streamlines.

Transonic data for two-element airfoil systems are scarce, and there are
little data at any speed where viscous effects are negligible. However, data
recently made available by the David Taylor Research and Development Center
have made possible the verification of the results of the method. The
airfoil-slat combination shown in figure 5 was designed for low-speed
application on a circulation control wing. The unconventional back end of
the main airfoil was designed to operate as a Coanda jet. A jet of high
velocity air is ejected tangentially along the upper surface near the trailing
edge of the main airfoil. The jet wraps around the rounded trailing edge
entraining the outer flow. The result is an airfoil system with a very
high circulation. The slat is deployed to prevent flow separation near the
leading edge of the main component. The case shown in figure 5 is for a low
Mach number, an angle of attack of 12°, and zero blowing. Because of the
small amount of aft loading, viscous effects on the main airfoil are small
and because of the high angle of attack there is very little separation on
the slat. As a result there is very good agreement between the computations
and the experimental data. Leading edge expansions are predicted correctly
on both elements. The only discrepancy is on the lower surface of the slat
where a small separation bubble is likely to exist. The lift coefficient on
this configuration is 1.83.

Blowing can be simulated in the computational method by shifting the rear stagnation point on the main airfoil away from its geometrical location toward the lower surface, as seen in figure 6. The location itself is chosen to match the circulation around the main airfoil. The streamline pattern in figure 6 has been computed for an angle of attack of 4.6° and a moderate amount of blowing. In this case the slat is practically aligned with the oncoming flow. The computed pressure coefficient distribution and the experimental data are compared in figure 7. Agreement in this case is even better. Now there is no flow separation on the lower surface of the slat, and there is good agreement in this region also. Leading edge peaks are correctly predicted and the large expansion near the trailing edge of the main component corresponding to the Coanda jet is also in agreement. The lift coefficient in this case is 4.70.

Unfortunately, not all airfoil systems are as free of viscous effects as this one. Therefore, the inviscid code has been coupled to a boundary layer program to account for viscous effects as described in reference 3. Consideration is presently limited to airfoil systems whose boundary layers do not merge but develop independently on each of the two airfoils. Boundary layer growth is computed using standard laminar and turbulent boundary layer methods. Transition points are either input or determined from empirical criteria, and checks are made for short and long bubble laminar separation. The presence of the boundary layer is accounted for in the outer inviscid flow by employing a surface source flow formulation for the boundary conditions as described by Lighthill (reference 5). The viscous flow over the airfoil system is then computed by solving iteratively for the outer inviscid flow and the boundary layer in a self-consistent fashion. At shock waves the computed pressure is smeared over a few mesh points and at the trailing edges the displacement thickness is extrapolated from upstream. Since separation is a frequent problem in multielement airfoil systems, a crude separated flow model has been incorporated into the program to enable it to run to completion. However, results in cases where the model is implemented are not necessarily accurate.

Results of computations with the viscous program are compared in figure 8 with experimental data obtained on another slat configuration tested at a Mach number of 0.649, and angle of attack of 4.6°, and a Reynolds number of 20 million. The agreement on the slat is not very good, but turbulent separation was predicted on the lower surface. The trend in the pressure is, however, correct, and the measured trailing edge pressure value is quite close to the predicted value. Because of the slenderness of the slat, separation on this element has little effect on the main airfoil. Agreement here is much better both on the upper and on the lower surface. In particular, the theory correctly predicts the multiple peaks in the pressures that have been measured near the leading edge. The flow accelerates to supersonic velocities, goes through a shock, and then quickly reaccelerates to supersonic speeds. This pattern is seen more clearly in figure 9 where some computed Mach line contours for this case are shown. To be noted are the supersonic region spanning the entire gap with the exit of the slot essentially sonic and the sonic bubble just behind it.

DESIGN OF TWO-ELEMENT AIRFOIL SYSTEMS

An analysis program can be of great help in the design of new airfoil configurations, but even so the analytical design could be a long process. The program would have to be run repeatedly with many contour modifications to achieve the desired flow characteristics. A computer program which could solve the inverse problem would indeed be valuable. An inverse program is one that generates the airfoil system that corresponds to a given pressure or velocity distribution. The development of such a program is currently underway. The approach to the inverse problem is that described by Tranen in reference 6 for the single airfoil design. The method consists of prescribing a desired velocity distribution on a starting airfoil system. The input velocities are integrated on each of the two airfoil surfaces to get the potential on the boundaries of the computational domain. The Dirichlet problem in the annulus is then solved and the normal component of velocity on the boundaries is computed. The boundaries are not necessarily streamlines now, but the computed normal velocities at the boundaries can be used to find nearby streamlines which are taken to be sought-after contours. This procedure is repeated until the normal velocity at the boundaries is driven to zero. But convergence is very fast. In the single airfoil design three or four iterations are usually sufficient. Of course, one could elect to design only one airfoil element or pieces of one or of both elements. In such cases a mixed boundary value problem needs to be solved, but this does not entail any additional numerical difficulties.

A difficulty with airfoil design is that no full solution of the inverse problem has ever been given, even for the case of incompressible flow over a single airfoil. The problem arises because there is no assurance that a physically acceptable airfoil shape will follow from an arbitrarily prescribed pressure distribution. For a given surface pressure distribution an airfoil will generally not close at the trailing edge and the upper and lower surfaces may intersect. Provisions have to be made to allow the achievable pressure distribution to vary somewhat from the initially prescribed values to obtain closure. Also it is probably true that if we wish to design both airfoil elements completely one will not be able to specify the pressure distribution on one element without taking into account the effect on this element due to the flow characteristics required on the second element. But this situation should not arise often in practice though. More likely will be the problem of redesigning only one of the airfoils or, even more commonly, only pieces of one element. This brings about the third type of design problem to be considered. In the case of a mixed design there are some regularity conditions that must be satisfied at the point where one switches from a geometry to a velocity boundary condition. This problem, as the trailing edge closure problem, is not unique to the two-element design, but is also present in the single airfoil design. It has not been dealt with satisfactorily even in this case.

CONCLUDING REMARKS

Beyond completion of the inverse code there are additional tasks that need to be undertaken to make the tools more useful to the designer. Melnik et al. have recently developed a more rational model for the viscous trailing edge. Its implementation in the analysis would certainly be an improvement. Also the viscous analysis code would have to be generalized to take into account the possibility of the boundary layers and/or wakes from the two elements merging as might be the case where the two elements are very closely spaced. In the design problem the desirable characteristics of a pressure distribution need to be determined. Clearly one wants shocks to be weak and to eliminate, or at least reduce, boundary layer separation. A bit harder to determine is what to design for, or try to achieve, on the surfaces along the slot between the two airfoils. Experimental data would serve as a useful guideline in this task. Shortcomings of previous designs and discrepancies between data and theory can give useful indications on which are the desirable pressure characteristics and which are the undesirable ones.

APPENDIX

SYMBOLS

A   radius of point of infinity in annular domain

C_ℓ lift coefficient

CP   pressure coefficient

C_μ blowing coefficient

M_∞ free-stream Mach number

r   radial direction in annular domain

R   radius of inner ring corresponding to secondary airfoil in annular domain

Re   Reynolds number

α angle of attack

θ azimuthal direction in annular domain

REFERENCES

1. Grossman, B. and Melnik, R.E., "The Numerical Computation of the Transonic Flow Over Two-Element Airfoil Systems," Proceedings of the Fifth International Conference on Numerical Methods in Fluid Mechanics, Springer-Verlag, pp. 220-237, June 1976.

2. Grossman, B. and Volpe, G., "An Analysis of the Inviscid Transonic Flow Over Two-Element Airfoil Systems," Office of Naval Research Report ONR-CR215-241-1, June 1977.

3. Grossman, B. and Volpe, G., "The Viscous Transonic Flow Over Two-Element Airfoil Systems," AIAA paper 77-688, June 1977.

4. Ives, D.C., "A Modern Look at Conformal Mapping, Including Doubly Connected Regions," AIAA Paper 75-842, June 1975.

5. Lighthill, M.J., "On Displacement Thickness," J. Fluid Mech. vol. 4, pp. 383-392, 1958.

6. Tranen, T.L., "A Rapid Computer Aided Transonic Airfoil Design Method," AIAA paper no. 74-501, June 1974.

7. Melnik, R.E., Chow, R., and Mead, H.R., "Theory of Viscous Transonic Flow Over Airfoils at High Reynolds Number," AIAA Paper 77-680, June 1977.
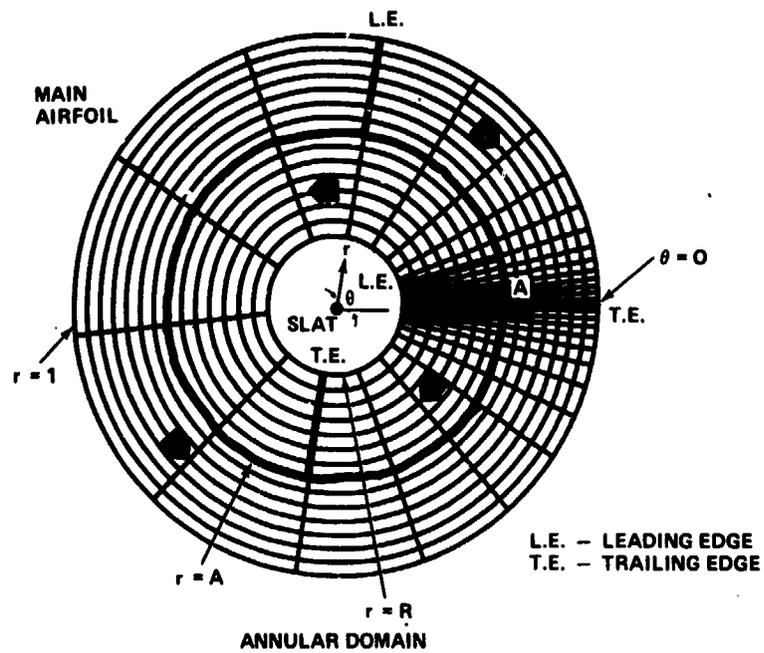
Figure 1.- Coordinate grid.
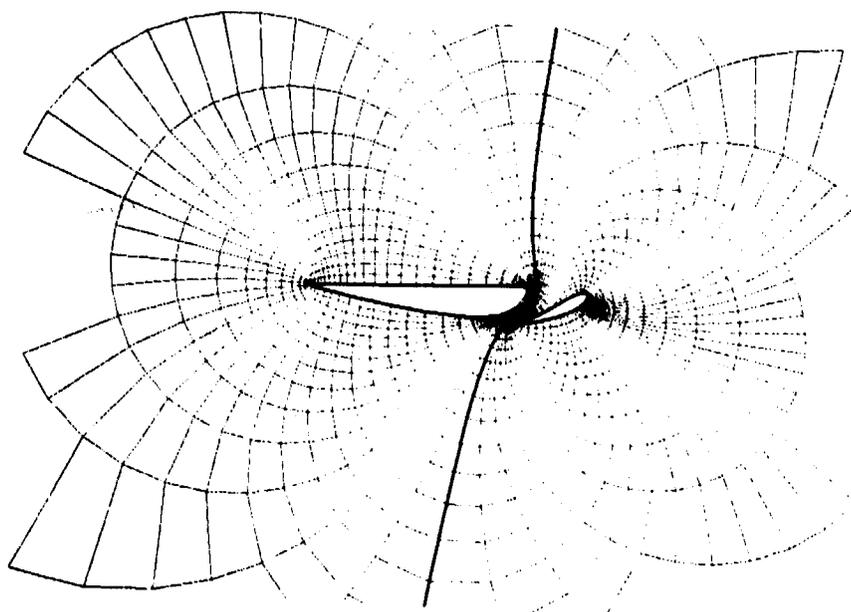
Figure 2.- Coordinate grid. Clark Y airfoil;
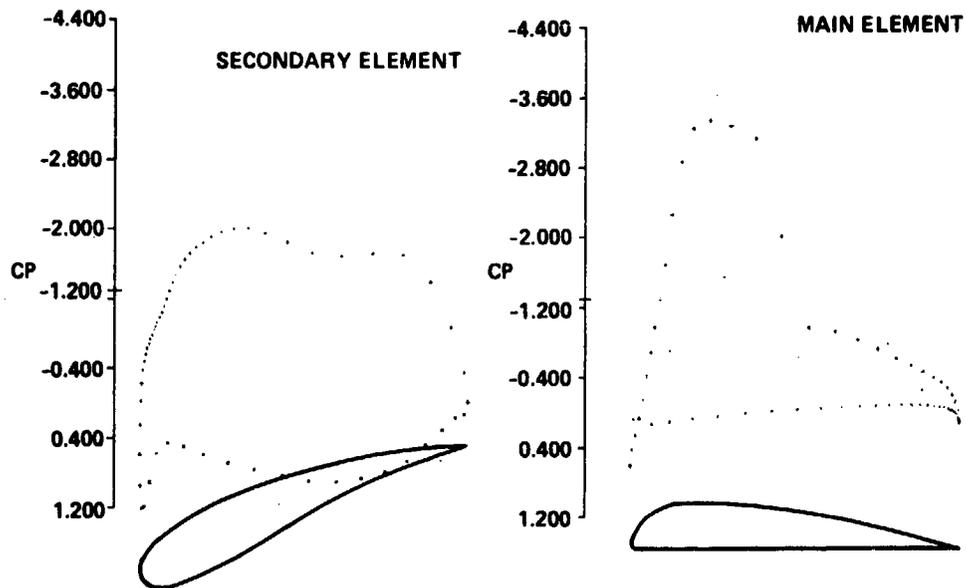30 percent Maxwell slat; 10 percent gap.

Figure 3.- Clark Y airfoil with 30 percent Maxwell slat.
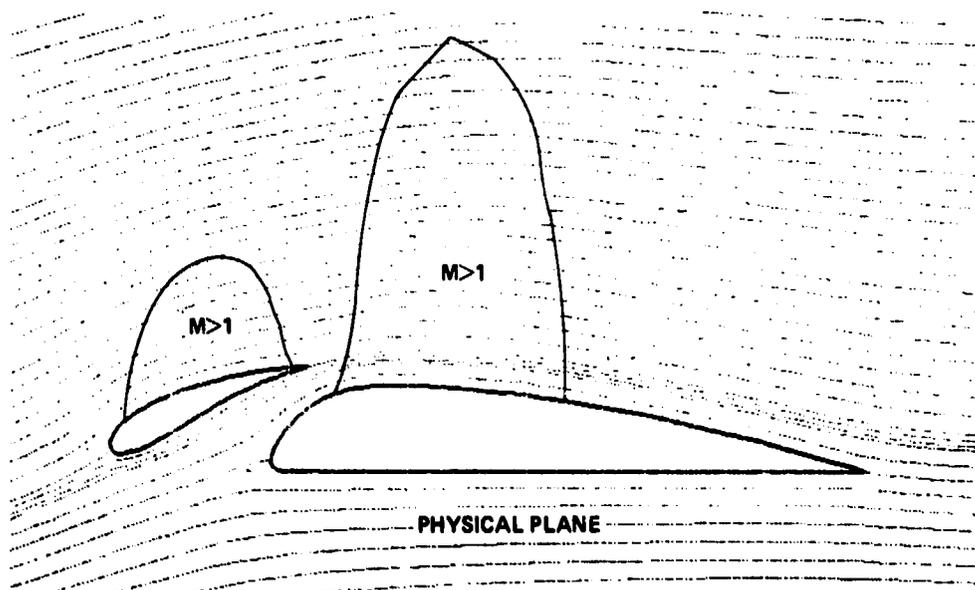$M_\infty = 0.6$; $\alpha = 6°$.

Figure 4.- Computed streamlines for Clark Y airfoil with 30 percent
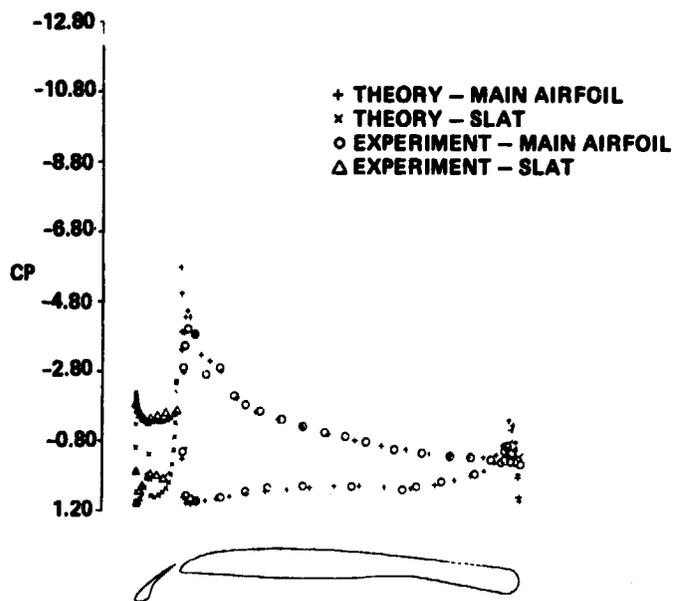Maxwell slat. $M_\infty = 0.6$; $\alpha = 6°$.

Figure 5.- Computed and experimental surface pressures on a CCW airfoil with 25° slat. $M_\infty = 0.1$; $\alpha = 12°$; $C_\mu = 0$.
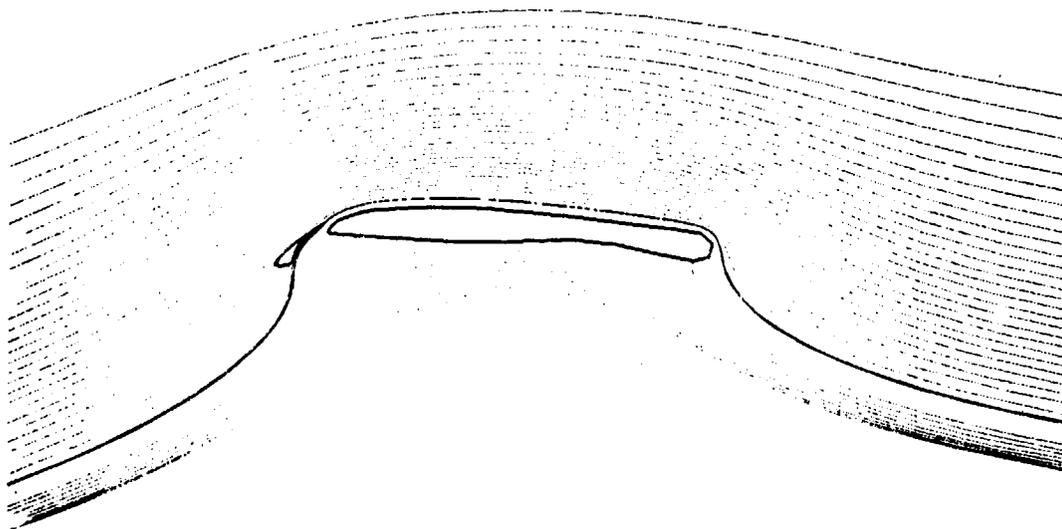

Figure 6.- Computed streamlines. CCW aifoil with 25° slat; $M_\infty = 0.1$; $\alpha = 4.6°$; $C_\mu = 0.1285$.

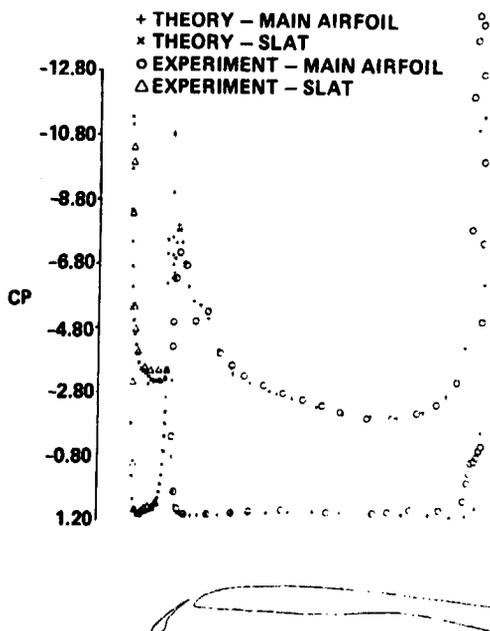Figure 7.– Computed and experimental surface pressures on a CCW airfoil with 25° slat. $M_\infty = 0.1$; $\alpha = 4.6°$; $C_\mu = 0.1285$.
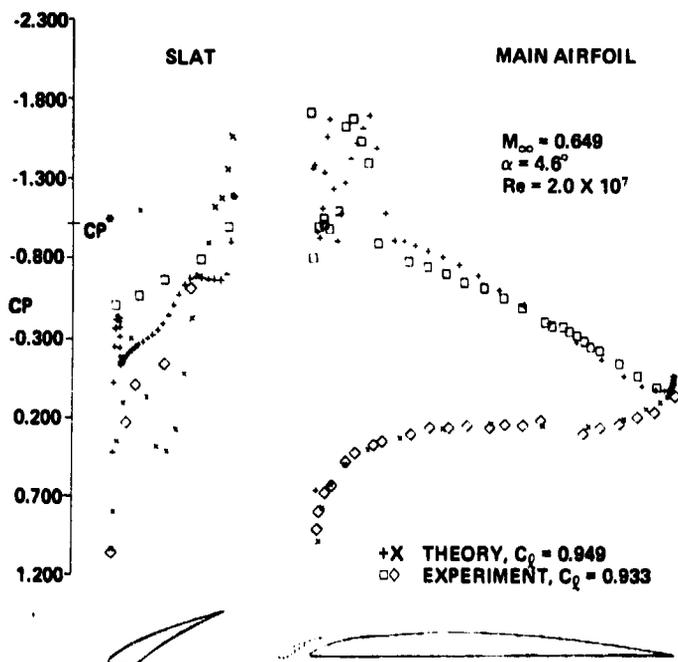

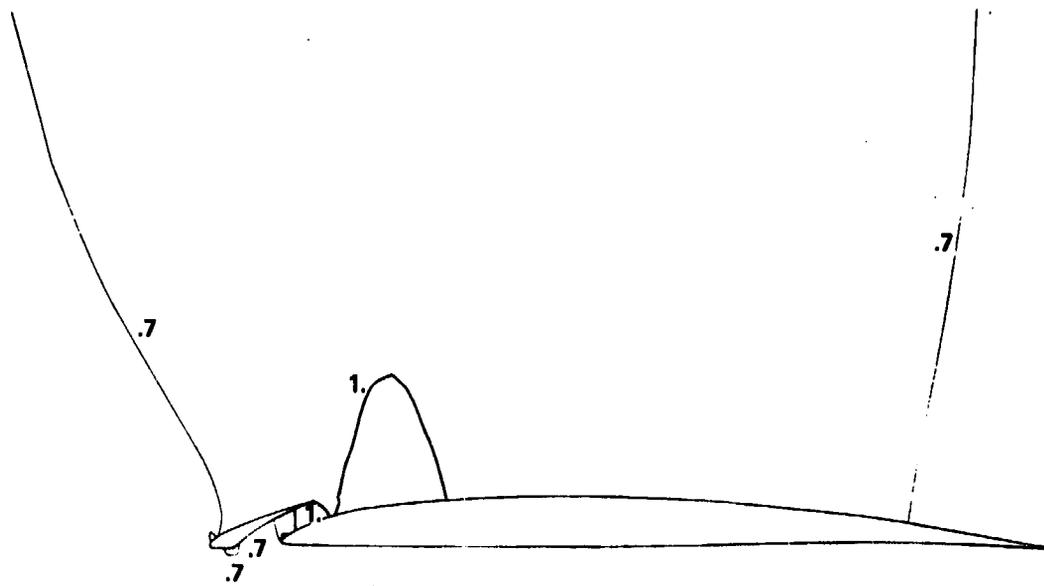Figure 8.– Computed and experimental surface pressures on an NACA 64A406 airfoil with 7.8A slat.

Figure 9.- Computed Mach number contours.   NACA 64A406 airfoil
with 7.8A slat; M_∞ = 0.649; α = 4.6°.